J Mater Sci: Mater Med (2011) 22:2239–2247
DOI 10.1007/s10856-011-4413-5

Preparation and characterization of temperature-responsive magnetic composite particles for multi-modal cancer therapy

Aihua Yao · Qi Chen · Fanrong Ai · Deping Wang · Wenhai Huang

Received: 6 April 2011 / Accepted: 1 August 2011 / Published online: 11 August 2011

Abstract The temperature-responsive magnetic composite particles were synthesized by emulsion-free polymerization of *N*-isopropylacrylamide (NIPAAm) and acrylamide (Am) in the presence of oleic acid-modified Fe_3O_4 nanoparticles. The magnetic properties and heat generation ability of the composite particles were characterized. Furthermore, temperature and alternating magnetic field (AMF) triggered drug release behaviors of vitamin B_{12}-loaded composite particles were also examined. It was found that composite particles enabled drug release to be controlled through temperature changes in the neighborhood of lower critical solution temperature. Continuous application of AMF resulted in an accelerated release of the loaded drug. On the other hand, intermittent AMF application to the composite particles resulted in an "on–off", stepwise release pattern. Longer release duration and larger overall release could be achieved by intermittent application of AMF as compared to continuous magnetic field. Such composite particles may be used for magnetic drug targeting followed by simultaneous hyperthermia and drug release.

A. Yao (✉) · Q. Chen · F. Ai · D. Wang · W. Huang
School of Materials Science and Engineering, Tongji University, Shanghai 200092, China
e-mail: aihyao@126.com

A. Yao · D. Wang · W. Huang
Key Laboratory of Advanced Civil Engineering Materials, Ministry of Education, Tongji University, Shanghai 200092, China

F. Ai
College of Mechanical and Electrical Engineering, Nanchang University, Nanchang Jiangxi 330031, China

1 Introduction

In recent years, mild hyperthermia treatment to tumor has attracted a lot of attention as an auxiliary method for treating cancer patients, especially when used in combination with other therapeutic methods such as radiotherapy and chemotherapy [1, 2]. It has been indicated that hyperthermia enhances apoptosis and the anti-tumor effects of chemotherapy through an increase in the uptake of carcinostatics into tumor cells, and inhibits the repair of tumor cell killing by anti-tumor drugs [3]. The dose of anti-tumor drugs, therefore, can be decreased by combination with hyperthermia, thus minimizing the undesirable side effects of chemotherapy drugs.

Conventional hyperthermia techniques including radio-frequency, microwave, water bath and hepatic perfusion suffer from several drawbacks such as insufficient coverage, poor temperature control and distribution, risk of organ damage, etc. [4, 5]. It is well known that heat can be generated by Néel relaxation, Brownian relaxation and hysteresis losses when magnetic nanoparticles are exposed to an alternating magnetic field (AMF), hence magnetic nanoparticles can be used as potential hyperthermia agents [6].

Magnetic nanoparticles are delivered to a tumor either intravenously or through direct injection. This is followed by application of an AMF that causes the nanoparticles to heat. As the temperature rises in nearby cancerous cells, they are eradicated due to rupture of the cellular membrane or denaturation of proteins [7]. Of the materials tested, iron oxide nanoparticles were the most promising because of their biocompatibility, heat generation ability and chemical stability [8].

Intelligent polymers which have the ability to respond to small external stimulus changes, such as temperature, pH,

photo field, and antigen have attracted significant attention, and a considerable number of studies have been undertaken [9–11]. Poly(*N*-isopropylacrylamide) (PNIPAAm) is a well-known temperature-sensitive polymer that exhibit lower critical solution temperature (LCST) slightly below body temperature, about ~32°C [12, 13]. The polymer chains of PNIPAAm undergo a coil (soluble)—globule (insoluble) transition when the external temperature cycles across the LCST. Thus, at a temperature below the LCST, PNIPAAm hydrogel absorbs water and exists in a swollen state, but it shrinks and displays an abrupt volume decrease when the environmental temperature is higher than the LCST. The LCST of the PNIPAAm can be tuned by incorporating co-monomer units, such as Am [12]. Such a temperature-responsive polymer with thermoreversible phase transition characteristics is attractive for biomedical and bioengineering applications [14, 15].

A combination of magnetic and temperature-responsive properties in the same composites are considered to increase the application potential for magnetic separation [16], nucleic-acid extraction and purification [17] and drug delivery [18], etc. Additionally, composite particles consisting of iron oxide core and temperature-responsive polymer shell can be loaded with anti-cancer drug, injected into the bloodstream, and targeted to the tumor using an external magnetic field gradient. When an AMF is applied after localization, the iron oxide magnetic cores of the composite particles generate heat, raising the temperature of the tumor and resulting in hyperthermia. At the same time, the heat generated is conducted form the core to the surrounding polymer and raise the temperature of the polymer shell above the LCST, trigger the release of the drug loaded in the polymer. In this way, the multi-modal cancer therapy, including drug targeting, drug delivery and hyperthermia will be achieved.

For this purpose, the magnetic composite particles consisting of iron oxide cores and temperature-responsive polymer shells were synthesized by emulsion-free polymerization, which were subsequently loaded with Vitamin B_{12} (that was used as model drug). Their magnetic properties and heat generation ability as well as in vitro drug release behavior under an AMF were investigated. In the present work, two different conditions, referred to as "continuous" and "intermittent", were applied, and the effect of the magnetic field on drug release profile was compared. The drug release profiles showed that longer release duration and larger overall release could be achieved by intermittent application of AMF as compared to continuous magnetic field. These investigations are rarely reported in related references. To obtain a desirable LCST, which should be slightly higher than the physiological temperature and lower than the LCST of the polymer, the copolymers formed of NIPAAm and Am with molar ratio of 15:1 were chosen.

2 Materials and methods

2.1 Materials

The monomer NIPAAm was obtained form J&K Chemica (99%) and recrystallized in n-hexane prior to use. Am, *N*,*N*-methylenebisacrylamide (MBAM), ammonium persulfate (APS), oleic acid, ferrous chloride hexahydrate ($FeCl_3{\cdot}6H_2O$) and iron sulfate heptahydrate ($FeSO_4{\cdot}7H_2O$) were obtained from Sinopharm Chemical Reagent Co., Ltd (China), Acrylamide was recrystallized from chloroform prior to use. All other materials were of analytical grade and used without further purification.

2.2 Synthesis of oleic acid-modified Fe_3O_4 nanoparticles

The oleic acid-modified Fe_3O_4 nanoparticles were synthesized based on co-precipitation method. Briefly, 2.36 g $FeCl_3{\cdot}6H_2O$ and 1.21 g $FeSO_4{\cdot}7H_2O$ were dissolved in 100 ml distilled water, and then 5 ml of concentrated ammonia was added to the solution rapidly with vigorous stirring under nitrogen atmosphere. Subsequently, 1.2 g oleic acid in 5 ml ethanol was added to above-mentioned solution. The mixed solution was heated to 70°C and kept at this temperature for 30 min, and the co-precipitation reaction took place. The magnetic particles thus formed were then separated by magnetic decantation and washed with hot ethanol several times to remove excess surfactant. The resultant particles were finally dispersed in 50 ml distilled water and pH was adjusted to 10 to yield stable magnetic fluid for further use.

2.3 Preparation of Fe_3O_4/P(NIPAAm-co-Am) composite particles

Fe_3O_4/P(NIPAAm-co-Am) composite particles were synthesized by emulsifier-free emulsion polymerization. Firstly, *N*-isopropylacrylamide-co-acrylamide, [P(NIPAAm-co-Am)], copolymers, were prepared. The total monomer concentration was adjusted to 0.02 mol/l and the molar ratio of NIPAAm and Am was 15:1 in the feed. 5 wt% MBAM (based on monomer weight) was added to the monomer mixture and stirred for 10 min. Various amount of Fe_3O_4 (5, 10 and 15% based on the monomer weight, designated as F5, F10, F15) were then added to the above-mentioned mixtures and purged with nitrogen for 30 min to remove oxygen. The solution was allowed to heat to 70°C,

and subsequently 3 wt% redox initiator, APS was added. After 7 h of reaction, the composite particles were separated by magnetic decantation. The resulting particles were finally washed with cold distilled water and dried at room temperature under reduced pressure for 24 h.

2.4 Characterization

The morphologies of oleic acid-modified Fe_3O_4 nanoparticles and Fe_3O_4/P(NIPAAm-co-Am) composite particles were observed with a Hitachi H-800 transmission electron microscopy (TEM) working at an accelerating voltage of 200 kV. Samples for TEM measurements were prepared by ultrasonically dispersing the particles into absolute ethanol, then placing a drop of the suspensions onto carbon-coated copper grids, and then drying in air. Fourier transform infrared (FTIR) analysis (Bruker EQUINOXSS, German) of the oleic acid-modified Fe_3O_4 nanoparticles and Fe_3O_4/P(NIPAAm-co-Am) composite particles were performed in the wavenumber range 400–4000 cm^{-1}, on disks prepared from a mixture of 2 mg samples and 150 mg of high-purity grade KBr. Temperature-responsive property of P(NIPAAm-co-Am) copolymer was characterized using a UV–visible spectrophotometer (JASCO V-570). Dynamic light scattering particle size analyzer (DLS, Autosizer 4700, Malvern Co.) was used to investigate particle size change of the composite particles. Magnetic property measurements were carried out at room temperature using a vibrating sample magnetometer (VSM, Model 4 HF, Nanjing University Instrument Plant, China) with a maximum field of 7×10^6 A/m. The polymer content of the composite particles was determined via thermogravimetric (TG, Netzsch STA 449 C) analysis. The concentration of vitamin B_{12} was determined in a UV–visible spectrophotometer (JASCO V-570).

2.5 Heat generation ability of the composite particles under an AMF

The heat generation ability of the composite particles was determined using a homemade experimental setup. The experimental setup consisted of three main parts: an alternation magnetic generator with frequencies ranging from 55 to 65 kHz and maximum amplitude of 1260 A/m (Nanjing University Instrument Plant, China), loops of induction coil and a thermally insulated glass container (double wall vacuum bottle). The composite particles with 15 wt% Fe_3O_4 nanoparticle loading were firstly allowed to fully swell in phosphate buffered solution (PBS) at 25°C. Subsequently, 20 mg samples were immersed into 1.0 ml deionized water placed in the thermally insulating glass container. An AMF (frequency 65 kHz and strength 6.5 kA/m) was applied to the samples through the coil. The temperature of water heated by the samples was monitored using an alcohol thermometer and was recorded with time.

2.6 Preparation of vitamin B_{12}-loaded composite particles

Vitamin B_{12} was used as model drugs for in vitro drug release study due to its high aqueous solubility and easy detection. Vitamin B_{12} was loaded onto the composite particles by incubating 100 mg of the dehydrated particles in 4 ml of vitamin B_{12} water solution (conc. 1 mg/ml) for 24 h at 25°C. After loading, the drug-loaded particles was separated by magnetic decantation, dried and stored under vacuum. The concentration of free vitamin B_{12} in the supernatant was determined by measuring the absorbance at 360 nm in a UV–visible spectrophotometer. The drug-loading efficiency was calculated as follows [18]:

$$\text{Drug - loading efficiency } (\%) = (W_{\text{feed}} - W_{\text{free}}) \times 100\%/W_{\text{feed}} \quad (1)$$

The drug-loading efficiency estimated using Eq. 1 was 65%.

2.7 Temperature triggered drug release

300 mg vitamin B_{12}-loaded composite particles were dispersed in 10 ml of PBS (pH 7.4) at 25°C, which was placed in a test tub with a closer. The test tube were placed in preheated water baths at 25°C (<LCST), physiological temperature (37°C, <LCST) or 42°C (>LCST). 4 ml of the release medium (free of particles) was extracted and replaced with a same volume of fresh PBS at predetermined time intervals (1, 4, 8, 12, 18 and 24 h). The amount of the free vitamin B_{12} in the extracted solution was quantified using UV–visible spectrophotometer and cumulative drug release was calculated. All drug release experiments were repeated at least three times.

2.8 AMF triggered drug release

AMF triggered drug release behaviors were performed under two different conditions, referred to as "continuous" and "intermittent". In the intermittent experiments, 300 mg of vitamin B_{12}-loaded composite particles were dispersed in 10 ml of PBS (pH 7.4) at 25°C, which was placed in a test tub with a closer. The test tube was then exposed to an AMF with strength of 6.5 kA/m and frequency of 65 kHz. The AMF was applied as a pulse for 1 h every 3 h, up to 24 h. On the other hand, for the continuous experiments, the samples were continuously subjected to the AMF for 24 h. For these two cases, after 24 h of exposure to an AMF, 4 ml of the release medium (free of

particles) was extracted and replaced with a same volume of fresh PBS at predetermined time intervals (1, 4, 8, 12, 18 and 24 h). The amount of the free vitamin B_{12} in the extracted solution was quantified using UV–visible spectrophotometer, and thus hourly release amount and cumulative drug release were calculated.

3 Results and discussion

3.1 Structure and morphology characterization

TEM images of the oleic acid-modified Fe_3O_4 nanoparticles and Fe_3O_4/P(NIPAAm-co-Am) composite particles were taken to determine their shapes, sizes and uniformities. As observed in Fig. 1a, the oleic acid-modified Fe_3O_4 nanoparticles are individually dispersed and uniform in shape and size, with an average diameter of $\sim$10 nm. Magnetic nanoparticles have a large ratio of surface area to volume, and therefore, tend to agglomerate in order to reduce their surface energy by strong dipole–dipole interactions and van der Waal's forces among particles [19]. The dispersion and stability of nanoparticles, however, can be improved by modifying the nanoparticles with a surfactant or a polymer. Among them oleic acid is usually used surfactant. Several authors have reported the magnetic iron oxide nanoparticles modified with oleic acid [20, 21]. In the present work, oleic acid molecules were chemisorbed to the surfaces of the magnetic nanoparticles, forming the first layer of surfactant. Subsequently excess oleic acid molecules were adsorbed to the first layer surfactant by hydrophobic interaction and form the second layer surfactant [20]. The outer layer of oleic acid molecules on the Fe_3O_4 surface reacted with NH_4OH solution and transformed into an ammonium salt, resulting in a good dispersibility of Fe_3O_4 nanoparticles in aqueous solution.

In the following experiments, the bilayer oleic acid-modified Fe_3O_4 nanoparticles were used as the seeds of emulsion polymerization. Under initiation of APS solution, the temperature-responsive P(NIPAAm-co-Am) copolymer chains were precipitated on the nanoparticles, and forming a core/shell structure. This was confirmed by TEM image of Fe_3O_4/P(NIPAAm-co-Am) composite particles as shown in Fig. 1b. Compared with the starting magnetite nanoparticles, a gray area of 20–30 nm in thickness surrounding the nanoparticles can be clearly observed after the polymer immobilization. It also can be seen in Fig. 1b that the composite particles are nearly spherical with an average diameter of $\sim$50 nm, but a small amount of agglomeration is detected. The agglomeration is probably due to the occurrence of crosslinking reaction between the particles.

Figure 2 shows FTIR spectra of the oleic acid-modified Fe_3O_4 nanoparticles and the Fe_3O_4/P(NIPAAm-co-Am) composite particles. The strong absorption bands at 2962, 2924 cm^{-1} (ν_{as}(C–H)), 2850 cm^{-1} (ν_s(C–H)), 1450 cm^{-1} ($\delta_{as}(CH)_3$), 1420 cm^{-1}($\delta_s(CH)_3$), and 1710 cm^{-1} (ν(C=O)) in Fig. 2a originate from oleic acid molecules. Another sharp band can be observed at 1640 cm^{-1}, which has been shift from 1710 cm^{-1} (C=O bond asymmetric vibration). This can be explained as the carboxyl groups of oleic acid combined with Fe atoms on the surface of Fe_3O_4 nanoparticles and rendered a partial single bone character of the C=O bond to weaken the bond, and then shifted the stretching frequency to a lower value [20]. The absorption bands at 630, 586 and 442 cm^{-1} are attributed to Fe–O from Fe_3O_4 nanoparticles [18]. The main characteristic absorption bands at 1640 and 1548 cm^{-1} corresponding to C=O (amide I) and N–H bending (amice II) are observed in Fig. 2b, indicating the temperature-responsive P(NIPAAm-co-Am) copolymer has been successfully coated on the surfaces of Fe_3O_4 nanoparticles. Furthermore, the coating was supported by the TGA plot presented in Fig. 3.

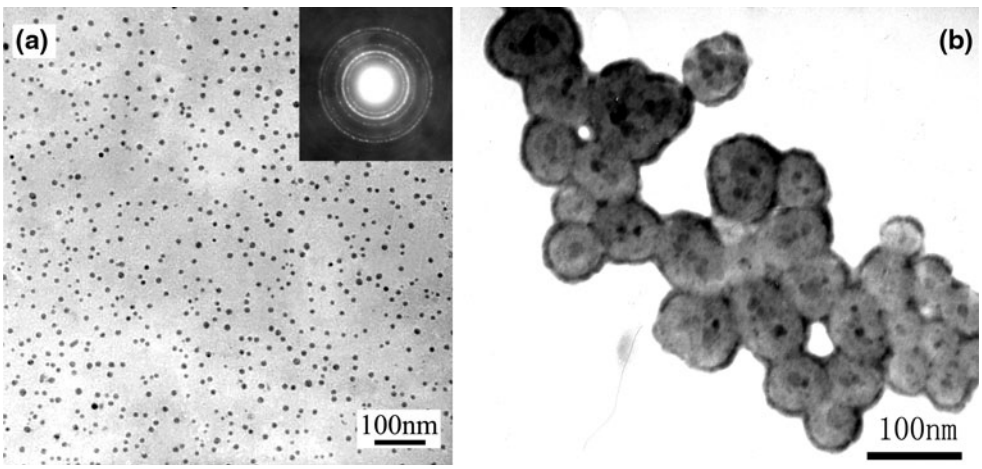

Fig. 1 TEM images of oleic acid-modified Fe_3O_4 nanoparticles (**a**) and Fe_3O_4/P(NIPAAm-co-Am) composite particles (**b**)

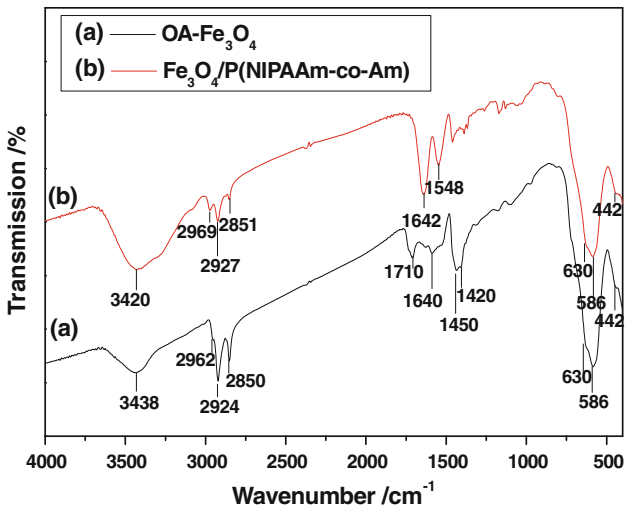

Fig. 2 FTIR spectra of oleic acid-modified Fe_3O_4 nanoparticles (*a*) and Fe_3O_4/P(NIPAAm-co-Am) composite particles (*b*)

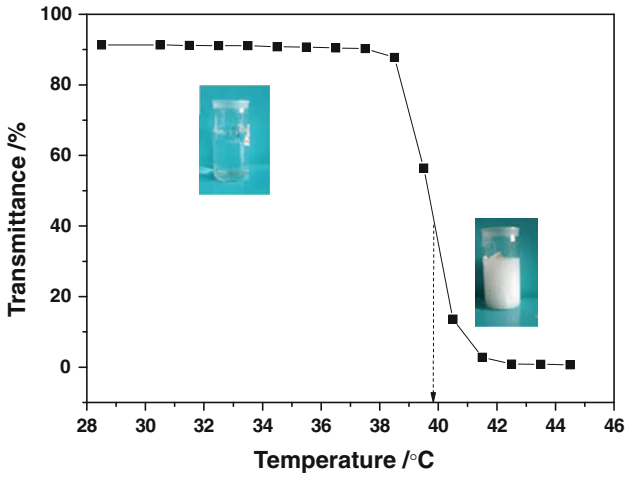

Fig. 3 LCST of P(NIPAAm-co-Am) copolymer measured by transmittance using a UV–visible spectrophotometer

The mass loss of 90 wt% on heating from 200 to 750°C implies that the drug carrier consists of 10 wt% of Fe_3O_4 nanoparticles and 80 wt% of the organic substances, including oleic acid and P(NIPAAm-co-Am) copolymer.

3.2 Temperature-responsive behavior of Fe_3O_4/P(NIPAAm-co-Am) composite particles

Temperature-responsive property of P(NIPAAm-co-Am) copolymer was characterized using a UV–visible photometer, and the LCST of the copolymer was determined from the curve of relationship between UV light absorbance and temperature [22]. As shown in Fig. 4, the 1 wt% copolymer solution changes from transparent to opaque at LCST of ~40°C. When the temperature-responsive polymer was

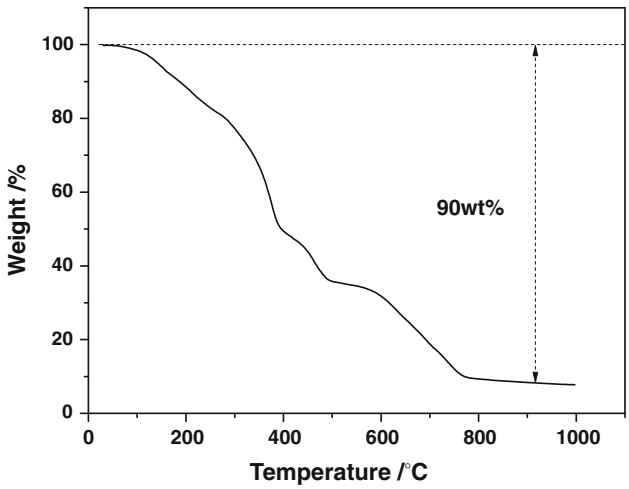

Fig. 4 TGA curve of the Fe_3O_4/P(NIPAAm-co-Am) composite particles

encapsulated on solid surfaces, the modified surface showed a hydrophilic-hydrophobic change because of the reversible hydration-dehydration of the polymer chains, which led to the size change of the composite particles. The DLS measurement result in Fig. 5 demonstrated the particle size change above and below the LCST. The diameters of the composite particles remain almost unchanged with temperature when the temperature is increased from 25 to 36°C. In contrary, when the temperature is raised to ~40°C, the diameters of the composite particles abruptly decrease from 235 to 197 nm, which suggests that the LCST of the magnetic composite particles is about 40°C. When the temperature was below 40°C, the hydrophilic copolymer chains stretched into water to separate every particle from its neighbors by steric force, while the temperature was above 40°C, the hydropholic copolymer chains collapsed on the surface of the composite nanoparticles. Due to the loss of steric force, composite nanoparticles got together to form big aggregates, resulting in the increase in the particle sizes. It was found that the particle size changed in a reversible manner in response to changes in temperature around their LCST (shown in Fig. 5 inset).

3.3 Magnetic property and heat generation ability

Figure 6 shows the hysteresis loops of oleic acid-modified Fe_3O_4 nanoparticles (Fig. 6d) and Fe_3O_4/P(NIPAAm-co-Am) composite particles with various magnetic nanoparticles loading (Fig. 6a–c) at room temperature. It is obvious that all samples show superparamagnetic behaviors. Saturation magnetization (*Ms*) of oleic acid-modified Fe_3O_4 nanoparticles is 75 emu/g, and the value significantly decreases upon encapsulating with P(NIPAAm-co-Am) copolymer. As observed, the *Ms* values are 9, 20 and

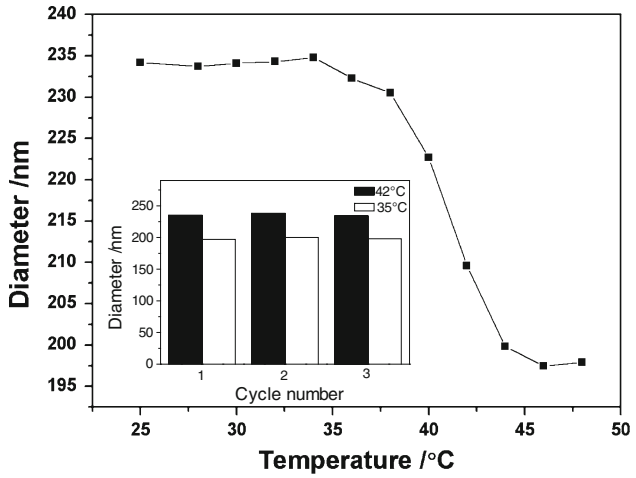

Fig. 5 Diameter of the Fe_3O_4/P(NIPAAm-co-Am) composite particles versus temperature curve obtained by DLS method. *Inset* shows the reversible change in particle size in response to temperature change (three heating–cooling cycles)

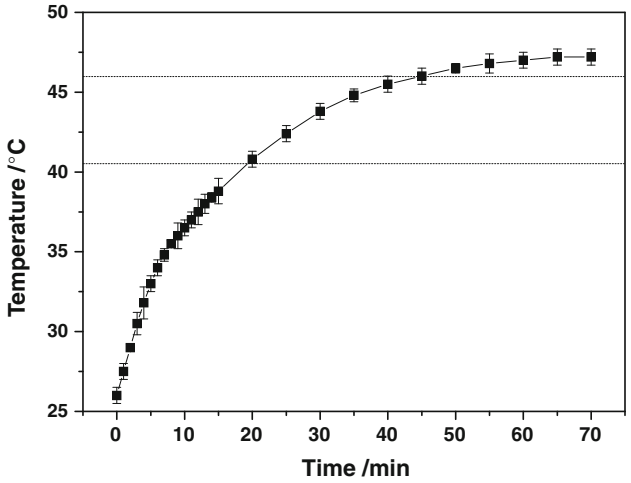

Fig. 7 Time-dependent temperature curve of composite particles with 15 wt% Fe_3O_4 loading in a 60 kHz and 6.5 kA/m magnetic field. *Dashed horizontal lines* indicate the hyperthermia temperature range of 41–47°C

23 emu/g for the samples F5, F10 and F15, respectively. The observed decrease in the magnetization value is primarily due to the reduced portion of magnetic material per mass of composite particles. In the copolymer-coated samples, there was less magnetic material per gram, and the magnetization readings were divided by substantial mass of copolymer [23].

In order to investigate the heat generation ability of the temperature-responsive magnetic composite particles, 50 mg as-synthesized samples were exposed to an external AMF of 65 kHz. The heating generated by samples under the AMF led to an increase in the temperature of distilled water. The deionized water temperature as a function of time for the composite particles with 15 wt% Fe_3O_4 nanoparticle loading is shown in Fig. 7. It is observed that the temperature of distilled water is elevated rapidly to 41°C in the first 20 min, and ultimately reaches an equilibrium temperature of 46°C in 60 min. The equilibrium temperature is higher than the LCST of P(NIPAAm-co-Am) copolymer. Therefore, it is believed that the present composite particles can be employed to regulate drug release via response to temperature change in the neighborhood of LCST by swelling and deswelling. Furthermore, the heating power generated by the magnetic nanoparticles is sufficient to meet the requirement of magnetic hyperthermia.

It should be pointed out here that the magnetic filed strength and frequency used in the present work is much lower than those reported in other literatures [24–26]. Hence, the heating generation ability of the composite particles can be enhanced by using higher magnetic field, which will subsequently increase the heating rate and reduce the dosage of the composite particles required for hyperthermia application.

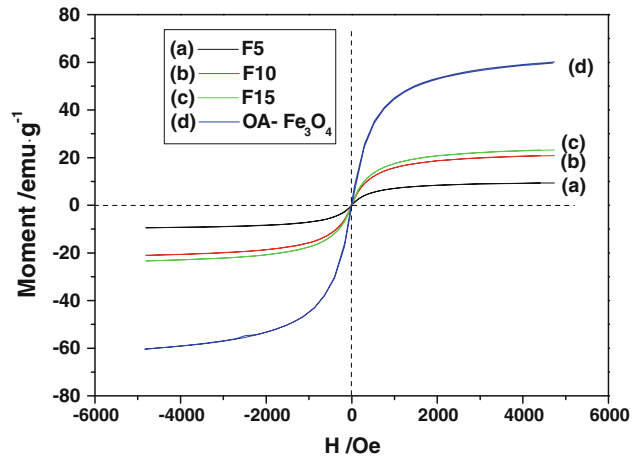

Fig. 6 Room-temperature hysteresis loops of the Fe_3O_4/P(NIPAAm-co-Am) composite particles with various magnetic nanoparticles loading (*a–c*) and oleic acid-modified Fe_3O_4 nanoparticles (*d*)

3.4 Temperature triggered drug release

To examine the temperature-triggered drug release ability of the vitamin B_{12}-loaded composite particles, three temperatures: room temperature (25°C) (<LCST), physiological temperature (37°C) (<LCST) and low hyperthermia temperature (42°C) (>LCST) were selected. The cumulative release of vitamin B_{12} from the composite particles was plotted with time. It can be seen from Fig. 8 in all cases, the release of vitamin B_{12} from the composite particles is relatively rapid during the initial 5 h, followed by a low rate of release. Additionally, the temperature-triggered drug release behavior is confirmed in Fig. 8. When the

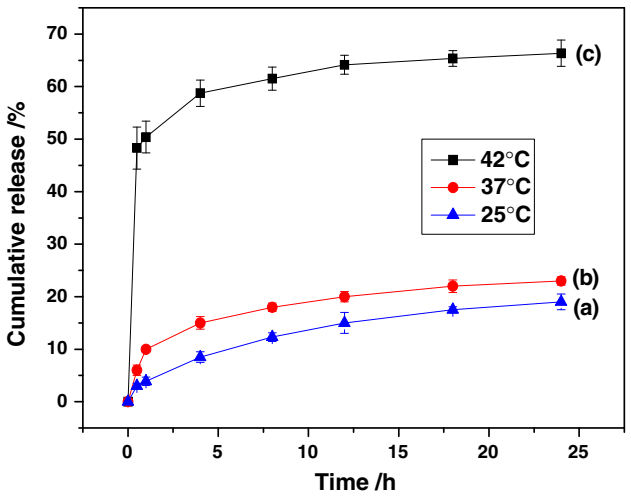

Fig. 8 Cumulative drug release profiles of vitamin B_{12}-loaded composite particles in PBS (pH 7.4) at 25°C, 37°C (<LCST) and 42°C (>LCST). The data points are the average of three experiments

temperature is below the LCST (25 and 37°C), the drug carrier is stable and the drug release is very low (<20%). However, when the temperature is higher than the LCST, the P(NIPAAm-co-Am) copolymer collapses such that the squeezing effect of the polymer leads to enhanced drug release [18]. Such a drug release behavior is especially suitable for multi-modal cancer therapy because it ensure that there is a near absence of drug release at the physiological temperature during the transport of drug, while there is fast or controlled drug release at slightly above the normal body temperature on arriving at the targeted tumor cells [18, 27–29].

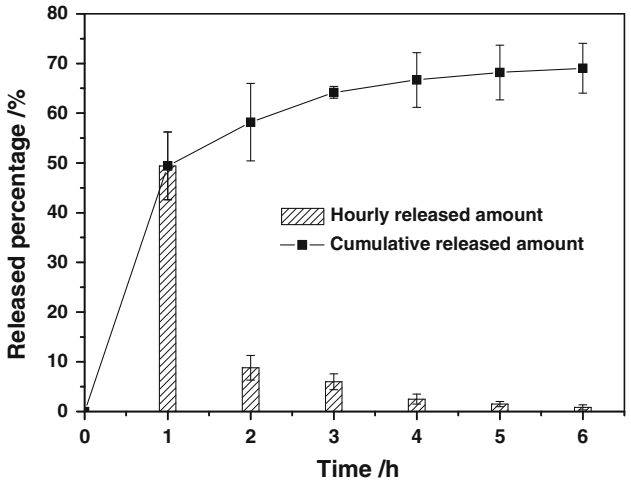

Fig. 9 Hourly released amount and cumulative release of vitamin B_{12} from the composite particles exposed to a continuous AMF of 60 kHz and 6.5 kA/m. The data points are the average of three experiments

3.5 AMF triggered drug release

AMF-triggered drug release behaviors of the vitamin B_{12}-loaded composite particles were performed under two different conditions, referred to as "continuous" and "intermittent". As shown in Fig. 9, continuous application of AMF leads to a fast release of vitamin B_{12} from the composite particles, with an overall drug release of 69% within 6 h. Also, an obvious initial burst release of ~50% in the first half hour is observed in Fig. 9. The above observations suggests that the heat generated by the magnetic field is transferred to the temperature-responsive polymer, raises the temperature of the polymer shell above its LCST, and as a result, trigger the release of the drug loaded in the polymer. Comparison of the release patterns of vitamin B_{12} in Figs. 8c and 9 shows that the drug release appears to be accelerated by application of an external magnetic field. It is speculated that higher temperatures (~46°C) were obtained by an AMF, and hence there were an enhancement in release rates due to increased drug diffusivity.

The hourly released amount and cumulative release of vitamin B_{12} from the composite particles are plotted in Fig. 10. It is obvious that an intermittent AMF application to the composite particles results in an "on–off", stepwise release pattern. With the magnetic field on, heat generated in the magnetic core raises the temperature of the drug-loaded polymer shell above its LCST, resulting in the shrinkage in volume of the composite particles and a corresponding burst release is observed. On the other hand, in the experiment with the magnetic field off, the polymer absorbs water and re-swells, and thus slows down the drug

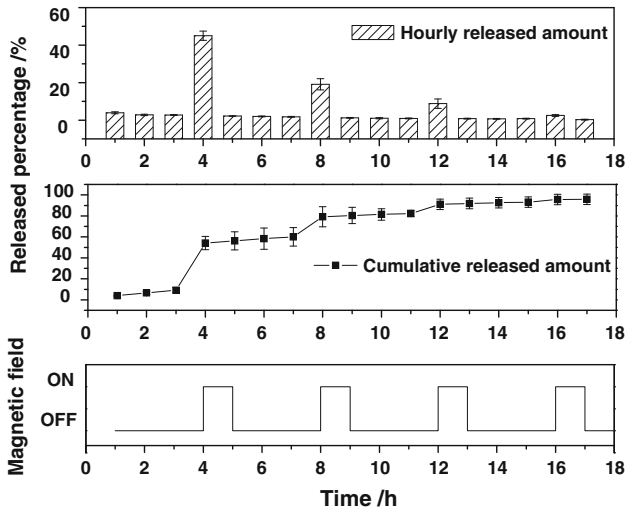

Fig. 10 Hourly released amount and cumulative release of vitamin B_{12} from the composite particles exposed to an intermittent AMF of 60 kHz and 6.5 kA/m. The AMF was applied as a pulse for 1 h every 3 h. The data points are the average of three experiments

release. Therefore, these composite particles are feasible for application in "on/off" drug delivery systems. The drug content in the composite particles decrease with time and hence limited actuation is achieved in the later stages. It was found almost complete drug release was observed after three on–off cycles in the present work.

The data from vitamin B_{12} release suggests that longer release duration and larger overall release can be achieved by intermittent application of AMF. However, the initial burst release is still high in this case, and thus limited release duration is achieved. In vivo application as drug delivery device typically needs release for weeks or months. It is, therefore, expected that essential modifications in the network structure of the polymer and the procedures for drug loading can lead to longer release durations. Additionally, manipulating the field magnitude and field exposure duration can tailor the burst release to desired magnitude and can even result in reduced release with prolonged AMF durations [30]. These various modifications will be taken into account in the subsequent research work, and related results will be reported in the near future.

4 Conclusions

Fe_3O_4/P(NIPAAm-co-Am) composite particles were prepared by emulsion free polymerization of NIPAAm and Am in the presence of oleic acid-modified Fe_3O_4 nanoparticles. DLS measurement showed the composite particles exhibited a LCST about 40°C. Additionally, the magnetic property measurements showed the heating power generated by the magnetic nanoparticles was sufficient to meet the requirement of magnetic hyperthermia. Temperature- and AMF-triggered drug release behaviors were confirmed. A marked difference in drug release rate was found at temperatures below and above the LCST of [P(NIPAAm-co-Am)] copolymers. At experimental temperatures lower than LCST, the drug release was very low. However, at temperatures higher than LCST, there was an initially rapid drug release followed by a low rate of release. The drug release profiles showed that longer release duration and larger overall release could be achieved by intermittent application of AMF as compared to continuous magnetic field. The multi-functional Fe_3O_4/P(NIPAAm-co-Am) composite particles may be considered as attractive implant materials for multi-modal cancer therapies.

Acknowledgments This work was financially supported by National Natural Science Foundation of China (No. 50702037) and the Scientific Research Foundation for the Returned Overseas Chinese Scholars, State Education Ministry.

References

1. Konishi K, Maehara T, Kamimori T, Aono H, Naohara T, Kikkawa H, Watanabe Y, Kawachi K. Heating ferrite powder with AC magnetic field for thermal coagulation therapy. J Magn Magn Mater. 2004;272–276:2428–9.
2. Issels RD. Hyperthermia adds to chemotherapy. Eur J Cancer. 2008;44:2546–54.
3. Itoh Y, Yamada Y, Kazaoka Y, Ishiguchi T, Honda N. Combination of chemotherapy and mild hyperthermia enhances the antitumor effects of cisplatin and adriamycin in human bladder cancer T24 cells in vitro. Exp Ther Med. 2010;1:319–23.
4. Purushotham S, Chang PEJ, Rumpel H, Kee IHC, Ng RTH, Chow PKH, Tan CK, Ramanujan RV. Thermoresponsive core-shell magnetic nanoparticles for combined modalities of cancer therapy. Nanotechnology. 2009;20:305101.
5. Moroz P, Jones SK, Gray BN. Magnetically mediated hyperthermia: current status and future directions. Int J Hyperth. 2002; 18:267–84.
6. Hergt R, Dutz S, Muller R, Zeisberger M. Magnetic particle hyperthermia: nanoparticles magnetism and materials development for cancer therapy. J Phys Condens Matter. 2006;18: 2919–34.
7. Day ES, Morton JG, West JL. Nanoparticles for thermal cancer therapy. J Biomech Eng Trans ASME. 2009;131:074001-1.
8. Gupta AK, Gupta M. Synthesis and surface engineering or iron oxide nanoparticles for biomedical applications. Biomaterials. 2005;26:3995–4021.
9. Zhang XZ, Yang YY, Chung TS, Ma KX. Preparation and characterization of fast response macroporous poly(*N*-isopropylacrylamide) hydrogels. Langmuir. 2001;17:6094–9.
10. Chen GH, Hoffman AS. Graft copolymers that exhibit temperature-induced phase transitions over a wide range of pH. Nature. 1995;373:49–52.
11. Miyata T, Asami N. A reversibly-antigen-responsive hydrogel. Nature. 1999;399:766–9.
12. Sershen SR, Westcott SL, Halas NJ, West JL. Temperature-sensitive polymer-nanoshell composites for photothermally modulated drug delivery. J Biomed Mater Res. 2000;51:293–8.
13. Ahmad H, Rahman MA, Jalil Miah MA. Magnetic and temperature-sensitive composite polymer particles and adsorption behavior of emulsifiers and trypsin. Macromol Res. 2008;16:637–43.
14. Shamim N, Hong L, Hidajat K, Uddin MS. Thermosensitive-polymer-coated magnetic nanoparticles: adsorption and desorption of bovine serum albumin. J Colloid Interface Sci. 2006;304: 1–8.
15. Ankareddi I, Brazel CS. Synthesis and characterization of grafted thermosensitive hydrogels for heating activated controlled release. Int J Pharm. 2007;336:241–7.
16. Sun YB, Ding XB, Zheng ZH, Cheng X, Hu XH, Peng YX. Magnetic separation of polymer hybrid iron oxide nanoparticles triggered by temperature. Chem Commun. 2006;22:2765–7.
17. Elaissari A, Rodrigue M, Meunier F, Herve C. Hydrophilic magnetic latex for nucleic acid extraction, purification and concentration. J Magn Magn Mater. 2001;225:127–33.
18. Zhang J, Misra RDK. Magnetic drug-targeting carrier encapsulated with thermosensitive smart polymer: core-shell nanoparticle carrier and drug release response. Acta Biomater. 2007;3:838–50.
19. Kohler N, Fryxell GE, Zhang MQ. A bifunctional poly(ethylene glycol) silane immobilized on metallic oxide-based nanoparticles for conjugation with cell targeting agents. J Am Chem Soc. 2004; 126:7206–11.
20. Lan Q, Liu C, Yang F, Liu SY, Xu J, Sun DJ. Synthesis of bilayer oleic acid-coated Fe_3O_4 nanoparticles and their application in

pH-responsive Pickering emulsions. J Colloid Inter Sci. 2007;310:260–9.
21. Sahoo Y, Pizem H, Fried T, Golodnitsky D, Burstein L, Sukenik CN, Markovich G. Alkyl phosphonate/phosphate coating on magnetic nanoparticles: a comparison with fatty acids. Langmuir. 2001;17:7907–11.
22. Wakamatsu H, Yamamoto K, Nakao A, Aoyagi T. Preparation and characterization of temperature-responsive magnetite nanoparticles conjugated with *N*-isopropylacrylamide-based functional copolymer. J Magn Magn Mater. 2006;302:327–33.
23. Vestal CR, Zhang ZJ. Synthesis and magnetic characterization of Mn and Co spinel ferrite-silica nanoparticles with tunable magnetic core. Nano Lett. 2003;3:1739–43.
24. Pradhan P, Giri J, Samanta G, Sarma HD, Mishra KP, Bellare J, Banerjee R, Bahadur D. Comparative evaluation of heating ability and biocompatibility of different ferrite-based magnetic fluids for hyperthermia application. J Biomed Mater Res B. 2007;81B:12–22.
25. Kuznetsov AA, Leontiev VG, Brukvin VA, Vorozhtsov GN, Kogan BY, Shlyakhtin OA, Yunin AM, Tsybin OI, Kuznetsov OA. Local radiofrequency-induced hyperthermia using CuNi nanoparticles with therapeutically suitable Curie temperature. J Magn Magn Mater. 2007;311:197–203.
26. Prasad NK, Rathinasamy K, Panda D, Bahadur D. *Tc*-tuned biocompatible suspension of $La_{0.73}Sr_{0.27}MnO_3$ for magnetic hyperthermia. J Biomed Mater Res B. 2008;85B:409–16.
27. Ketlef MS, Thomas SR. Thermosensitive magnetic polymer particles as contactless controllable drug carriers. J Magn Magn Mater. 2006;302:267–71.
28. You YZ, Hong CY, Pan CY, Wang PH. Synthesis of a dendritic core-shell nanoparticles with a temperature-sensitive shell. Adv Mater. 2004;16:1953–7.
29. Choi SW, Zhang Y, Xia YN. A temperature-sensitive drug release system based on phase-change materials. Angew Chem Int Ed. 2010;49:7904–8.
30. Satarkar NS, Hilt JZ. Magnetic hydrogel nanocomposites for remote controlled pulsatile drug release. J Control Rel. 2008; 130:246–51.